

Asymptotic behaviour of the number of self-avoiding walks on finitely ramified fractals

This article has been downloaded from IOPscience. Please scroll down to see the full text article.

1994 J. Phys. A: Math. Gen. 27 7739

(<http://iopscience.iop.org/0305-4470/27/23/017>)

View [the table of contents for this issue](#), or go to the [journal homepage](#) for more

Download details:

IP Address: 171.66.16.68

The article was downloaded on 01/06/2010 at 22:19

Please note that [terms and conditions apply](#).

Asymptotic behaviour of the number of self-avoiding walks on finitely ramified fractals

Sava Milošević† and Ivan Živić‡

† Faculty of Physics, University of Belgrade, PO Box 550, 11001 Belgrade, Serbia, Yugoslavia

‡ Faculty of Natural Sciences and Mathematics, University of Kragujevac, 34000 Kragujevac, Serbia, Yugoslavia

Received 23 June 1994, in final form 18 October 1994

Abstract. We study self-avoiding walks (SAWs) on the checkerboard (CB) family of fractals, each member of which can be labelled by an odd integer b ($3 \leq b < \infty$), so that the fractal dimension d_f tends to the Euclidean value 2 when $b \rightarrow \infty$. By applying the exact renormalization-group method (for $b = 3, 5$ and 7), and the Monte Carlo renormalization-group method (for a sequence of fractals with $5 \leq b \leq 81$), we have calculated the critical exponent γ , associated with the total number of distinct SAWs. It turns out that γ , being always larger than the corresponding Euclidean value $\frac{43}{32}$, increases monotonically with b . In order to learn the asymptotic behaviour of γ for large b , we have applied the finite-size scaling (FSS) method (based on previous exact results for wedges of the two-dimensional Euclidean lattices), and thereby we have shown that γ tends to $\frac{103}{32}$ from below, when $b \rightarrow \infty$. Applying the same method (FSS), we have also demonstrated that the critical exponent ν , associated with the mean-squared end-to-end distance of SAWs, tends to the Euclidean value $\frac{3}{4}$ from below, when $b \rightarrow \infty$. The obtained results extend, and in a way weld together, the previous studies of SAWs on various families of finitely ramified fractals.

1. Introduction

The self-avoiding walk (SAW) on a lattice is a random walk whose path must not contain self-intersections. For a large number of steps N , the number of distinct SAWs (averaged over all possible starting points) is governed by the power law $C_N \sim \mu^N N^{\gamma-1}$, where μ is the connectivity constant, and γ is the related critical exponent. In the case of SAWs on two-dimensional Euclidean lattices the value $\gamma = \frac{43}{32}$ [1] has been recognized as a universal value, whereas in the case of fractal lattices (embedded in the two-dimensional Euclidean space) it has turned out that γ can take a wide variety of values. Consequently, γ has to be calculated for each new fractal studied. More interestingly, for two infinite fractal families embedded in the two-dimensional Euclidean space, it has been found [2, 3] that when the fractal properties (the fractal d_f and spectral d_s dimensions) approach the corresponding Euclidean values, γ does not tend to $\frac{43}{32}$. Thus, in the case of the Sierpinski gasket (SG) family of fractals, whose members are labelled by an integer b ($2 \leq b < \infty$), the known values of γ (for $2 \leq b \leq 80$) increase monotonically with b [2], and the finite-size scaling (FSS) approach [4] revealed that $\gamma \rightarrow \frac{133}{32}$ when $b \rightarrow \infty$. Similarly, in the case of the plane-filling (PF) family of fractals, whose members are enumerated by an odd integer b ($3 \leq b < \infty$), the calculated values of γ (for $3 \leq b \leq 121$) also increase monotonically with b [3], and the FSS analysis [3] showed that $\gamma \rightarrow \frac{103}{32}$ when $b \rightarrow \infty$. Accordingly, one

may question whether the monotonic departure from the Euclidean value $\frac{43}{32}$ is a general characteristic of γ for SAWs on finitely ramified fractals.

In this paper we study SAWs on the checkerboard (CB) family of fractals, whose members are finitely ramified and can be enumerated by the odd integer b ($3 \leq b < \infty$). The corresponding renormalization-group (RG) calculation of γ is more intricate than in the SG and PF case. Nevertheless, we have succeeded in obtaining exact values of γ for fractals with $3 \leq b \leq 7$. To get γ for larger b we have applied the Monte Carlo renormalization-group (MCRG) approach, and in this way we have reached all values of γ up to $b = 81$ (the evaluation of the last one, for $b = 81$, took 11 days of continuous work, as a solely processed job on a computer with the Intel 80860 microprocessor). In relation to the asymptotic behaviour of γ for SAWs on the CB fractals, we have applied the FSS method, and thereby we have learnt that $\gamma \rightarrow \frac{103}{32}$ when $b \rightarrow \infty$. Besides, to establish values of γ for $3 \leq b \leq 81$ it was necessary to use results related to the critical exponent ν (associated with the SAW end-to-end distance). These results for ν (for finite b) were recently obtained via an exact and MCRG approach [5, 6]. However, within the corresponding studies [5, 6], the asymptotic behaviour of ν (for large b) was not established. In the course of the present work, we have been able to implement a specific FSS method and to learn that ν approaches the Euclidean value $\frac{3}{4}$, when $b \rightarrow \infty$, in the same way as in the case of the SG and PF families of fractals, that is, with the same correction term $\ln \ln b / \ln b$. Consequently, as regards both the critical exponent γ and ν , one can say that this work makes complete a long series of studies of SAWs on the three (SG, PF, and CB) infinite families of finitely ramified fractals (previous results and the new results are compared and reviewed in the discussion section of this paper).

This paper is organized as follows. In section 2 we present the general framework of the RG method for studying SAWs on the CB fractals, in a way that should make the method transparent for exact calculations, as well as for the Monte Carlo (MC) calculations, of the SAW critical exponents. In section 3 we give specific results for the critical exponent γ for a sequence of the CB fractals with $3 \leq b \leq 81$, while in section 4 we apply the FSS method to learn asymptotic behaviour of γ (and ν) for large b . Discussion of the obtained results and their relevance to the current knowledge of statistics of SAWs on fractals are given in section 5. Finally, in the appendix we provide details of the RG analysis which were not expounded in section 2.

2. Framework of the renormalization-group calculation of the critical exponent γ

The RG calculation of γ for SAWs on the CB fractals is, in principle, similar to the previous applications of the RG method to the studies of SAWs on other families of finitely ramified fractals. However, the implementation of the RG method for the CB fractals is more complex and requires additional elucidation. Before going into requisite details, we shall briefly describe the structure of the CB fractals, as well as the closely related family of the X fractals. Each member of the plane CB and X family is labelled by an odd integer $b \geq 3$ and can be obtained as the result of an infinite iterative process of successive ($r \rightarrow r + 1$) enlarging the fractal structure b times and substituting the smallest parts of the enlarged structure with the generator (initial structure, $r = 1$). The generator of a CB fractal is a square, of size $b \times b$, composed of b rows of unit squares, so that within each row and each column every other of them is removed, whereas in the case of X fractals instead of unit squares we put crosses composed of squares' diagonals (see, for instance, figure 1 of [5], and figure 1 of [6]). Guided by the self-similar way of the construction of the fractals, one

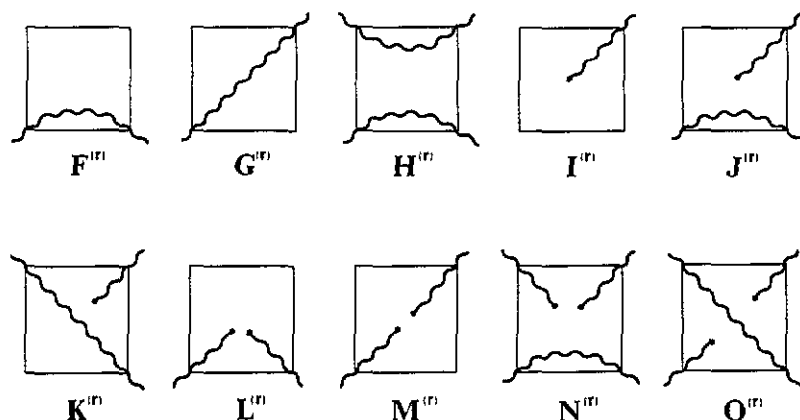


Figure 1. Schematic representation of the ten restricted partition functions (for an r th stage fractal construction) used in the calculation of the SAW critical exponent γ . The interior structure of the r th-order fractal triangle is not shown (its presence is represented by the wiggles of the SAW paths).

can easily show that the fractal dimension d_f for an arbitrary CB fractal (as well as for X), specified by b , is equal to $\ln[(b^2 + 1)/2]/\ln b$ (whereupon, one can observe that d_f tends to 2 when $b \rightarrow \infty$).

In order to study the number of all possible SAWs on the CB (X) fractals, it is necessary to introduce ten restricted partition functions (see figure 1). The first three restricted partition functions, that is, $F^{(r)}$, $G^{(r)}$, and $H^{(r)}$, comprise a RG which allows one to find the end-to-end distance critical exponent ν [5, 6]. The corresponding RG transformations are the recursion relations of the polynomial type

$$\begin{aligned}
 F^{(r+1)} &= \sum_{i,j,k} A_b(i, j, k) F^{(r)i} G^{(r)j} H^{(r)k} \\
 G^{(r+1)} &= \sum_{i,j,k} B_b(i, j, k) F^{(r)i} G^{(r)j} H^{(r)k} \\
 H^{(r+1)} &= \sum_{i,j,k} C_b(i, j, k) F^{(r)i} G^{(r)j} H^{(r)k}
 \end{aligned} \tag{1}$$

which gives the critical exponent

$$\nu = \frac{\ln b}{\ln \lambda_1} \tag{2}$$

where λ_1 is the largest eigenvalue of the RG transformations linearized at the non-trivial fixed point.

The additional seven restricted partition functions satisfy the following set of recursion relations:

$$\begin{aligned}
 X^{(r+1)} &= a_{XI} I^{(r)} + a_{XJ} J^{(r)} + a_{XK} K^{(r)} \quad X = I, J, K \\
 Y^{(r+1)} &= b_{II}^Y (I^{(r)})^2 + b_{IJ}^Y I^{(r)} J^{(r)} + b_{IK}^Y I^{(r)} K^{(r)} + b_{JJ}^Y (J^{(r)})^2 + b_{JK}^Y J^{(r)} K^{(r)} + b_{KK}^Y (K^{(r)})^2 \\
 &\quad + b_{LL}^Y L^{(r)} + b_{MM}^Y M^{(r)} + b_{NN}^Y N^{(r)} + b_{OO}^Y O^{(r)} \quad Y = L, M, N, O
 \end{aligned} \tag{3}$$

where the coefficients a and b (except b_L^0 , b_M^0 , and b_N^0 , which are always equal to zero) are polynomials in $F^{(r)}$, $G^{(r)}$, and $H^{(r)}$. All these functions, together with the corresponding initial conditions (expressed in terms of the fugacity x [5]), are necessary to construct the generating function $C(x) = \sum_{N=1}^{\infty} C_N x^N$, whose singular behaviour at the critical fugacity $x^* = 1/\mu$ is described by the critical exponent γ (in accordance with the assumption that the number of all possible walks of N steps is governed by the power law $C_N \sim \mu^N N^{\gamma-1}$). It can be verified that $C(x)$ is of the form

$$C_b(x) = \sum_{r=0}^{\infty} \left(\frac{2}{b^2 + 1} \right)^{r+1} \{ p_{II} (I^{(r)})^2 + p_{IJ} I^{(r)} J^{(r)} + p_{IK} I^{(r)} K^{(r)} \\ + p_{JJ} (J^{(r)})^2 + p_{JK} J^{(r)} K^{(r)} + p_{KK} (K^{(r)})^2 \\ + p_L L^{(r)} + p_M M^{(r)} + p_O O^{(r)} + p_N N^{(r)} \} \quad (5)$$

where the coefficients p are also polynomials in $F^{(r)}$, $G^{(r)}$ and $H^{(r)}$. The above form for $C(x)$ springs from the fact that all possible SAW paths, within the $(r+1)$ th-order fractal structure, can be made in ten different ways. This form shows that the behaviour of $C(x)$, in the vicinity of x^* , depends on the corresponding behaviour of the restricted partition functions. Assuming that the singular behaviour of (5) is of the form $C(x) \sim (x^* - x)^{-\gamma}$, it can be shown that the following relation holds:

$$\gamma = \frac{\ln(2\lambda_2^2/(b^2 + 1))}{\ln \lambda_1} \quad (6)$$

where λ_2 is the largest eigenvalue of the 3×3 matrix formed of the coefficients a^* (which appear in the RG transformations (3)) evaluated at the non-trivial fixed point of the RG transformations (1), that is, λ_2 is the solution of the equation

$$\begin{vmatrix} (a_{II}^* - \lambda_2) & a_{IJ}^* & a_{IK}^* \\ a_{JI}^* & (a_{JJ}^* - \lambda_2) & a_{JK}^* \\ a_{KI}^* & a_{KJ}^* & (a_{KK}^* - \lambda_2) \end{vmatrix} = 0. \quad (7)$$

To verify (6), an intricate analysis is necessary, and we present the relevant details in the appendix. Here we note that to learn specific values of γ , for particular members of the CB fractal family, one needs to calculate λ_2 (values of λ_1 have already been found for a set $3 \leq b \leq 81$ [5, 6]).

3. Exact and MCRG results for γ

An exact calculation of γ requires knowledge of coefficients of polynomials a which appear in (3). They can be calculated by enumerating the entire set of possible SAWs which are described by the restricted partition functions $I^{(r)}$, $J^{(r)}$, and $K^{(r)}$ (see figure 1). We have found that this enumeration is feasible in the case $b = 3, 5$ and 7 . More precisely, for $b = 3$ the enumeration can be done straightforwardly, whereas for $b = 5$ and 7 it necessitated a computer facility (which produced very large sets of data, which are available upon request from the authors). The values obtained for γ are given in table 1.

For a sequence of $b \geq 9$, the exact determination of polynomials a cannot be reached using present-day computers. However, to calculate λ_2 one does not need a complete knowledge of polynomials a (that is, one does not need to know all their coefficients). In

Table 1. The exact ($b = 3, 5$, and 7) and the MCRG ($5 \leq b \leq 81$) results for the RG eigenvalue λ_2 and the SAW critical exponent γ . To make the table complete we quote values of λ_1 (and ν) [6] that were used in formula (6) to calculate γ . Results are the same for the CB and X fractals for all b , except for the $b = 3$ case. As regards the exact RG and MCRG findings, we can comment that the results for $b = 5$ and $b = 7$ indicate that the deviation is not larger than 0.11%.

b	No of MC simulation	λ_1	λ_2	ν	γ
3	Exact (CB)	3	5.1213	1	1.5086
	Exact (X)	3	5	1	1.4650
5	Exact	6.6105	15.4410	0.85235	1.5403
	5×10^5	6.61 ± 0.04	15.5 ± 0.1	0.85216 ± 0.00304	1.542 ± 0.016
7	Exact	10.8869	34.7817	0.81502	1.6248
	5×10^5	10.87 ± 0.06	34.7 ± 0.4	0.81552 ± 0.00199	1.623 ± 0.014
9	Exact	15.8172	—	0.79578	—
	5×10^5	15.81 ± 0.09	65 ± 1	0.79594 ± 0.00167	1.677 ± 0.016
11	5×10^5	21.3 ± 0.1	110 ± 2	0.78338 ± 0.00142	1.726 ± 0.017
13	5×10^5	27.3 ± 0.1	169 ± 5	0.77532 ± 0.00124	1.759 ± 0.019
15	5×10^5	33.9 ± 0.2	249 ± 8	0.76850 ± 0.00115	1.791 ± 0.021
19	5×10^5	48.2 ± 0.2	480 ± 20	0.75980 ± 0.00098	1.843 ± 0.024
23	5×10^5	64.5 ± 0.3	850 ± 50	0.75261 ± 0.00092	1.901 ± 0.031
25	5×10^5	73.1 ± 0.4	1040 ± 60	0.75002 ± 0.00086	1.899 ± 0.030
27	5×10^5	82.2 ± 0.4	1400 ± 100	0.74756 ± 0.00084	1.936 ± 0.036
35	5×10^5	120.3 ± 0.6	2800 ± 400	0.74221 ± 0.00082	1.972 ± 0.057
43	5×10^5	164.1 ± 0.7	5400 ± 700	0.73742 ± 0.00060	2.030 ± 0.050
51	5×10^5	212 ± 1	9000 ± 2000	0.73371 ± 0.00079	2.064 ± 0.103
61	5×10^5	275 ± 1	14000 ± 4000	0.73196 ± 0.00067	2.054 ± 0.102
71	5×10^5	346 ± 1	23000 ± 4000	0.72910 ± 0.00050	2.090 ± 0.065
81	5×10^5	420 ± 2	40000 ± 10000	0.72765 ± 0.00056	2.143 ± 0.102

fact, to obtain λ_2 , one only needs values of these polynomials at the fixed point (see (7)). On the other hand, the polynomials which appear in (3) can be conceived as grand partition functions of appropriate ensembles, and consequently, within the MCRG method [2, 3], the requisite values of polynomials can be determined directly. Details of the way to ascertain values of a are quite similar to the way applied previously [2, 3], and here we will not elaborate on it further. In table 1 we present our findings for γ and λ_2 for a sequence of the CB fractals ($5 \leq b \leq 81$). From the table, it follows that γ , being always larger than $\frac{43}{32}$, increases monotonically with b (in the interval studied). Therefore, one may ask what happens for $b > 81$, and, in particular, what happens in the case $b \rightarrow \infty$, when the CB fractal dimension approaches the Euclidean value 2. We investigate the matter related to this question in the next section.

4. The finite-size scaling analysis

If we want to know the behaviour of γ for large values of b , we cannot avoid having to find out the asymptotic behaviour of ν . Indeed, according to (6), in order to determine γ we need to study both λ_1 and λ_2 when $b \rightarrow \infty$, which we are going to do. But, knowing the behaviour of λ_1 , one can learn the behaviour of ν through (2).

We start with an analysis of the RG transformations (1) for large b . First, we observe that it was established [6] that the probability of the H type of SAW (see figure 1) vanishes for large b , which means that the function $H^{(r)}$ can be neglected. For the remaining two

functions, we write the following short expressions:

$$F^{(r+1)} = f_b(F^{(r)}, G^{(r)}) \quad (8)$$

$$G^{(r+1)} = g_b(F^{(r)}, G^{(r)}) \quad (9)$$

and introduce two new quantities $\epsilon_F^{(r)}$ and $\epsilon_G^{(r)}$ through

$$F^{(r)} = F_\infty^* \exp(\epsilon_F^{(r)}) \quad (10)$$

$$G^{(r)} = G_\infty^* \exp(\epsilon_G^{(r)}). \quad (11)$$

The new quantities should measure closeness to the fixed point (F_∞^*, G_∞^*) which is pertinent to the case $b \rightarrow \infty$ (the corresponding critical fugacity we denote by x_∞^*). For the sake of simplicity, we shall omit the superscript r in writing the quantities ϵ_F and ϵ_G . To assess the asymptotic behaviour of (8) and (9), it is useful to recall their analogy with the corner-spin–corner-spin correlation functions (see figure 1) of the n -vector model (for $n = 0$). For this reason we assume, in the spirit of the FSS method [4], the two scaling forms

$$F^{(r+1)} \approx \frac{K_F}{b^a} \exp(\psi_F(\epsilon_F b^{1/\nu}, \epsilon_G b^{1/\nu})) \quad (12)$$

$$G^{(r+1)} \approx \frac{K_G}{b^a} \exp(\psi_G(\epsilon_F b^{1/\nu}, \epsilon_G b^{1/\nu})) \quad (13)$$

which should be valid for large b and small ϵ_F and ϵ_G . Here K_F and K_G are constants, while ψ_F and ψ_G are the scaling functions. The quantity a is the critical exponent which governs the power-law decay of the correlation functions with distance. For large b , assuming the case of a wedge of the Euclidean square lattice with opening angle α equal to $\pi/2$, one may accept

$$a = \frac{\alpha}{2} \quad (14)$$

which can be inferred from the previous studies of SAWs on the Euclidean lattices' wedges [7, 8].

The scaling functions ψ_F and ψ_G are not known for arbitrary b . However, it is possible to deduce their forms for large b . Actually, for large b the inequality $x_b^* > x_\infty^*$ holds (because the lattice connectivity increases with increasing b). For $x > x_\infty^*$, the functions $F^{(r+1)}$ and $G^{(r+1)}$, given by (12) and (13), should vary as $\exp(b^2)$ [9], which implies the following form for the scaling functions:

$$\psi_F(y_F, y_G) \approx K_1 y_F^{2\nu} + K_2 y_G^{2\nu} \quad (15)$$

$$\psi_G(y_F, y_G) \approx K_3 y_F^{2\nu} + K_4 y_G^{2\nu} \quad (16)$$

where K_i ($i = 1, 2, 3$ and 4) are some constants. Knowing the last two expressions, we proceed to find the fixed point of the RG transformations (12) and (13). To this end, we combine the latter two with (10) and (11), which yields

$$a \ln b \approx \psi_F(y_F^*, y_G^*) \quad (17)$$

$$a \ln b \approx \psi_G(y_F^*, y_G^*). \quad (18)$$

Inserting (15) and (16) in the above two formulae (with $y_F^* = \epsilon_F^* b^{1/\nu}$ and $y_G^* = \epsilon_G^* b^{1/\nu}$) we find

$$\epsilon_F^* \approx (Q_F a \ln b)^{1/2\nu} b^{-1/\nu} \tag{19}$$

$$\epsilon_G^* \approx (Q_G a \ln b)^{1/2\nu} b^{-1/\nu} \tag{20}$$

where $Q_F = (K_4 - K_2)/(K_1 K_4 - K_2 K_3)$ and $Q_G = (K_1 - K_3)/(K_1 K_4 - K_2 K_3)$. The requisite eigenvalue λ_1 should be determined by solving the equation

$$\begin{vmatrix} \frac{\partial F^{(r+1)}}{\partial F^{(r)}} - \lambda_1 & \frac{\partial F^{(r+1)}}{\partial G^{(r)}} \\ \frac{\partial G^{(r+1)}}{\partial F^{(r)}} & \frac{\partial G^{(r+1)}}{\partial G^{(r)}} - \lambda_1 \end{vmatrix}^* = 0 \tag{21}$$

where the asterisk means that all derivatives should be taken at the fixed point given by (19) and (20). Thus we find

$$\lambda_1(b) \approx Q b^{1/\nu} (a \ln b)^{(2\nu-1)/2\nu} \tag{22}$$

where Q is a constant. Using (2) and (22) we get the formula for the critical exponent

$$\nu(b) = \frac{3}{4} - \frac{3}{16} \frac{\ln \ln b}{\ln b} \tag{23}$$

which is asymptotically correct for large b . One can notice that ν acquires the Euclidean value $\frac{3}{4}$ for $b \rightarrow \infty$ (with the negative first correction term). This result was anticipated in [6], on the grounds of predictions given in [4]. In fact, one could have reached the same result (23) in an easier way, that is, by assuming that the scaling functions (15) and (16) are equal, which would make the whole approach identical to the approach of [4]. However, such an assumption would imply that the coefficients $A_b(i, j, k)$ and $B_b(i, j, k)$ which appear in (1) are mutually proportional (for large b), which at the present stage lacks numerical and physical evidence. Anyhow, we can now conclude that ν has the same type of behaviour for the three different (SG, PF, and CB) families of fractals.

We proceed to find asymptotic behaviour of the critical exponent γ . For this purpose, we first need to determine asymptotic behaviour for the eigenvalue λ_2 , which should be accomplished by solving (7) for large b . In the case of large b , it is known [4, 8, 10] that the three-leg vertex partition functions $J^{(r)}$ and $K^{(r)}$ can be neglected in comparison with the one-leg vertex partition function $I^{(r)}$, on which grounds (7) can be reduced to

$$\lambda_2(b) \approx a_{II}(F_b^*, G_b^*, b). \tag{24}$$

In the spirit of the FSS approach, and in the analogy with (12) and (13), we assume

$$a_{II}(F_\infty^* \exp(\epsilon_F), G_\infty^* \exp(\epsilon_G), b) \approx K b^c \exp(\psi_a(\epsilon_F b^{1/\nu}, \epsilon_G b^{1/\nu})) \tag{25}$$

where K is a constant, c is an appropriate critical exponent, and ψ_a is the scaling function. The specific value of c can be determined by an analysis of the polynomial a_{II} as a function of the fugacity x . For $x < x_\infty^*$ (that is, for $\epsilon_F < 0$ and $\epsilon_G < 0$) the polynomial a_{II} diverges according to the power law

$$a_{II} \sim (x_\infty^* - x)^{-31/64} \tag{26}$$

which springs from the study [7] of SAWs confined in the Euclidean wedges (taking into account that in the case under study the opening angle α is $\pi/2$). The scaling assumption (25), in conjunction with the power law (26), can be valid if

$$\psi_a(\epsilon_F b^{1/\nu}, \epsilon_G b^{1/\nu}) = -\frac{31}{64} \ln(\epsilon_F b^{1/\nu} + \epsilon_G b^{1/\nu}) \quad (27)$$

and accordingly

$$c = \frac{31}{48}. \quad (28)$$

In the next step, we analyse a_{II} for $x > x_\infty^*$ (for the densed phase) so as to learn $\lambda_2(b)$ for large b . In this case the ratio of $a_{II}/F^{(r+1)}$ should be a definite function of b [4, 8]. More specifically, one can expect

$$\frac{a_{II}(F_\infty^* \exp(\epsilon_F), G_\infty^* \exp(\epsilon_G), b)}{F^{(r+1)}(F_\infty^* \exp(\epsilon_F), G_\infty^* \exp(\epsilon_G), b)} \sim b^\omega h(x - x_\infty^*) \quad (29)$$

where the exponent ω depends on the opening angle α of the Euclidean wedge, and h is a function which does not depend of b . For $\alpha = \pi/2$, following the work of Duplantier and Saleur [8], we have found

$$\omega = \frac{31}{16}. \quad (30)$$

On the other hand, (29) together with (12) and (25) imply

$$\psi_a(y_F, y_G) - \psi_F(y_F, y_G) = \ln(C_1 y_F^{(\omega-a-c)\nu} + C_2 y_G^{(\omega-a-c)\nu}) \quad (31)$$

where C_1 and C_2 are constants. Hence, for the fixed-point values (19) and (20) we get

$$\ln \lambda_2(b) \approx (a+c) \ln b + \frac{1}{2}(\omega-a-c) \ln \ln b. \quad (32)$$

Finally, using (6), (22) and (32), we obtain

$$\gamma(b) = 2\nu(a+c+1) + \nu(\omega-a-c - (2\nu-1)(a+c-1)) \frac{\ln \ln b}{\ln b} \quad (33)$$

and, using the specific findings, we reach the asymptotic expression

$$\gamma(b) = \frac{103}{32} - \frac{219}{128} \frac{\ln \ln b}{\ln b} \quad (34)$$

which shows the non-Euclidean value ($\frac{103}{32}$ versus $\frac{43}{32}$) for the critical exponent γ in the limit $b \rightarrow \infty$, when the fractal dimension d_f acquires the Euclidean value 2.

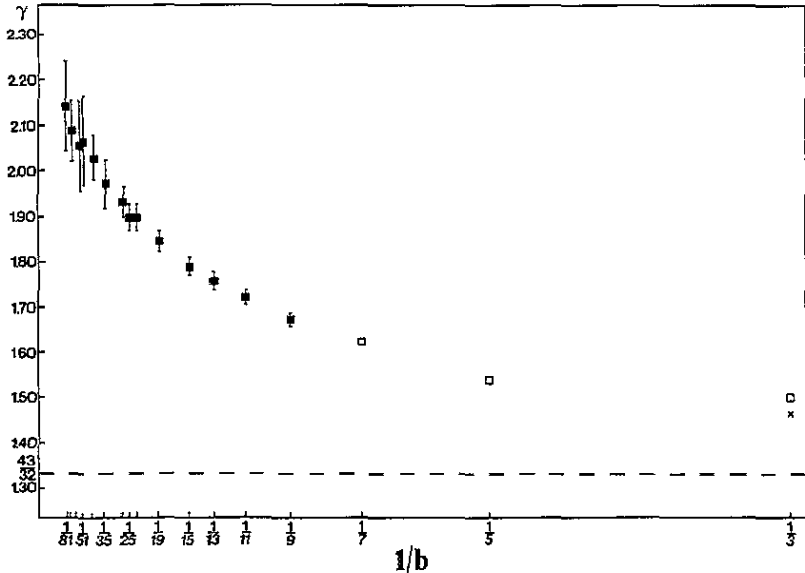


Figure 2. The exact (open squares) and MCRG (full squares) results for the critical exponent γ of SAWs on the CB fractals (the mark \times denotes the $b = 3$ exact value for the X fractal). The horizontal broken line represents the Euclidean value $\gamma = \frac{43}{32}$. This figure vividly demonstrates that the data from table 1 increases monotonically with b , always being larger than the Euclidean value $\frac{43}{32}$. In addition, one can see that it would be rather difficult to extrapolate straightforwardly the existing data to the asymptotic value $\frac{103}{32}$ (for $b \rightarrow \infty$) which has been obtained by an independent theoretical method (see section 4).

5. Discussion and conclusions

The initial objective of this work was to obtain values for the critical exponent γ of SAWs on the fractals which belong to the CB and X families of fractals. This objective has been accomplished by applying the exact RG method for the first three members ($b = 3, 5$ and 7) of the families, and by applying the MCRG method for a set of fractals with $5 \leq b \leq 81$. The results obtained are given in table 1, and here we depict γ as a function of $1/b$ in figure 2. One can observe that γ , being always larger than the Euclidean value $\frac{43}{32}$, increases monotonically with b , and one may wonder what happens for $b > 81$. We have answered this question via the FSS approach, which led us to the conclusion that $\gamma \rightarrow \frac{103}{32}$ when $b \rightarrow \infty$ (see formula (34)). Very similar behaviour of γ , and the same limiting value of $\frac{103}{32}$, has been found in the case of the PF family of fractals [3]. This equality of the limiting values should not be surprising since in both cases the $b = \infty$ fractal can be related to the wedge of the square lattice with the opening angle $\alpha = \pi/2$ [7, 10]. Incidentally, results for the PF fractals show that one can hardly expect a well defined function of dimension (exclusively) which interpolates results for critical exponents of SAWs on the Euclidean lattices and on fractal lattices [11]. In fact, all PF fractals (with the odd integer enumerator $3 \leq b < \infty$) have the same fractal dimension $d_f = 2$ and separate values of γ (and ν) for each b .

In fulfilling our task of calculating γ we have found it possible to answer the appealing question [6] about the large- b behaviour of the critical exponent ν for the CB fractals. Within the framework of the FSS approach, we have been able to learn that ν tends to the Euclidean value $\frac{3}{4}$ from below, when $b \rightarrow \infty$ (see formula (23)). This finding, together with the

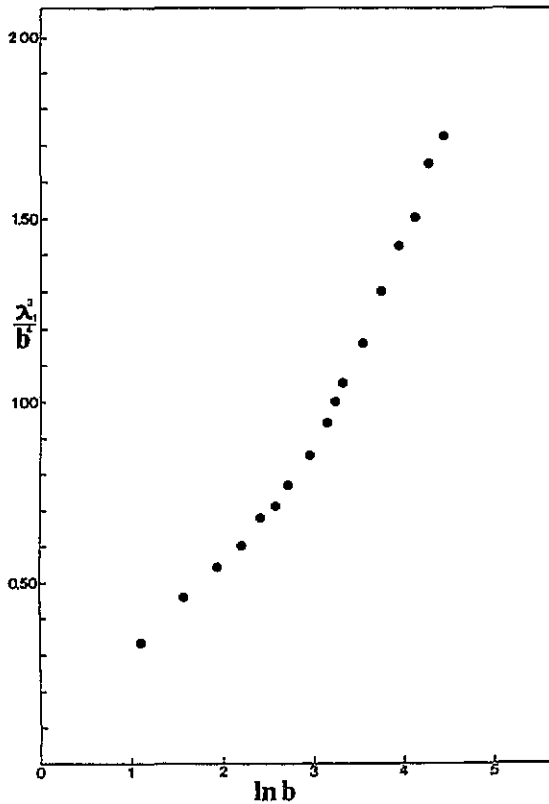


Figure 3. The graphical representation of the results given in table 1, depicted so as to disclose that λ_1^3/b^4 should be a linear function of $\ln b$ for large b .

previous results for ν (in the interval $3 \leq b \leq 81$) [6], which showed that ν decreases monotonically (passing through the value $\frac{3}{4}$ at $b \approx 25$), imply that ν , as a function of b , should have a minimum at some finite $b > 81$. Therefore, although the results for finite b and the $b \rightarrow \infty$ prediction are obtained theoretically by different approaches, we can try to locate the position of the minimum using (22), according to which λ_1^3/b^4 should be a linear function of $\ln b$, for large b . Indeed, the corresponding plot of our data (see table 1) gives the graph presented in figure 3, from which one can notice that the linear behaviour can be expected for $b > 27$. Therefore, making the least-squares fit to our data for $b > 27$, we have found $\lambda_1^3/b^4 = 0.65675 \ln b - 1.17595$, which upon inserting in (2) brings about an approximate function $\nu(b)$ with the minimum $\nu_{\min} \approx 0.71835$ located at $b_{\min} \approx 1750$. This estimate for b_{\min} is of the same order of magnitude as the one $b_{\min} \approx 1800$ found, using phenomenological formulae for ν , in the case of the PF fractals [3]. These values of b are beyond the reach of the MCRG method (implemented on present-day computers) and further analysis of the location of ν_{\min} requires new insights.

We have already pointed out that this work completes and welds together a set of related studies [2–6, 12, 13] of SAWs on four different families of fractals, and in this spirit we can offer the following conclusions. The critical exponent γ turns out to be always larger than the Euclidean value $\frac{43}{32}$, and, as a function of the fractal scaling factor b , increases monotonically with b . In the case of the SG family of fractals $\gamma \rightarrow \frac{133}{32}$ when $b \rightarrow \infty$, whereas for the other three families (PF, CB, and X) $\gamma \rightarrow \frac{103}{32}$ when $b \rightarrow \infty$. On the contrary, the critical exponent ν , for all four families of fractals, tends to the Euclidean value $\frac{3}{4}$ (from below), when the fractal dimensions approach the Euclidean value 2, that is, in the limit

$b \rightarrow \infty$. Besides, in all four cases ν is a non-monotonic function of b , so that it crosses the Euclidean value $\frac{3}{4}$ for a finite $b_h \approx 26$ [6], which appears to be the first universal element in the critical behaviour of SAWs on fractals. From the practical point of view, this means that there is a borderline in the homogeneity of fractals (embedded in the two-dimensional Euclidean space), such that for less homogeneous fractals ν is larger than the Euclidean value $\frac{3}{4}$, while for more homogeneous fractals ν lies below $\frac{3}{4}$. The first possibility, $\nu \geq \frac{3}{4}$, seems to be widely accepted, whereas the second, $\nu < \frac{3}{4}$, is less appreciated, although it has been observed in other investigations, both numerically [14] and experimentally [15]. The particular position of the apparently universal borderline, $b_h \approx 26$, is enhanced by the results reported in the present work. Indeed, one can notice, upon comparison with the results found previously [2,3], that for $b > 25$ (and up to $b = 81$) ν acquires values that are, within the error bars, almost the same for the four families of fractals.

Acknowledgments

We would like to acknowledge helpful correspondence with D Dhar during the course of the work presented in this paper. We would also like to thank V Matić for providing the possibility of an extensive use of the requisite computer facility.

Appendix.

Here we present an analysis that in its final stage vindicates the central formula (6). We start with examining the singular behaviour of the generating function (5) for the values $x = x^* - \delta$, where δ is a small positive number. To this end we linearize the RG transformations (1) at the non-trivial fixed point

$$\begin{pmatrix} F^{(r+1)} - F^* \\ G^{(r+1)} - G^* \\ H^{(r+1)} - H^* \end{pmatrix} = \begin{pmatrix} \frac{\partial F^{(r+1)}}{\partial F^{(r)}} & \frac{\partial F^{(r+1)}}{\partial G^{(r)}} & \frac{\partial F^{(r+1)}}{\partial H^{(r)}} \\ \frac{\partial G^{(r+1)}}{\partial F^{(r)}} & \frac{\partial G^{(r+1)}}{\partial G^{(r)}} & \frac{\partial G^{(r+1)}}{\partial H^{(r)}} \\ \frac{\partial H^{(r+1)}}{\partial F^{(r)}} & \frac{\partial H^{(r+1)}}{\partial G^{(r)}} & \frac{\partial H^{(r+1)}}{\partial H^{(r)}} \end{pmatrix}^* \begin{pmatrix} F^{(r)} - F^* \\ G^{(r)} - G^* \\ H^{(r)} - H^* \end{pmatrix} \tag{A1}$$

which can be written in the condensed form

$$\mathbf{u}^{(r+1)} = \hat{\mathbf{T}}\mathbf{u}^{(r)}. \tag{A2}$$

We assume that the vicinity of the fixed point is reflected in the smallness of the $\mathbf{u}^{(r)}$ intensity

$$|\mathbf{u}^{(r)}| \leq \epsilon \ll 1. \tag{A3}$$

Assuming that \mathbf{e}_1 is the eigenvector associated with the largest eigenvalue λ_1 of the matrix $\hat{\mathbf{T}}$, we shall make the approximation $\mathbf{u}^{(r)} \simeq \alpha(r, \delta)\mathbf{e}_1$, so that (A2) implies $\alpha(r, \delta) = \lambda_1^r \alpha(0, \delta)$ and

$$\mathbf{u}^{(r)} \simeq \alpha(0, \delta)\lambda_1^r \mathbf{e}_1 \tag{A4}$$

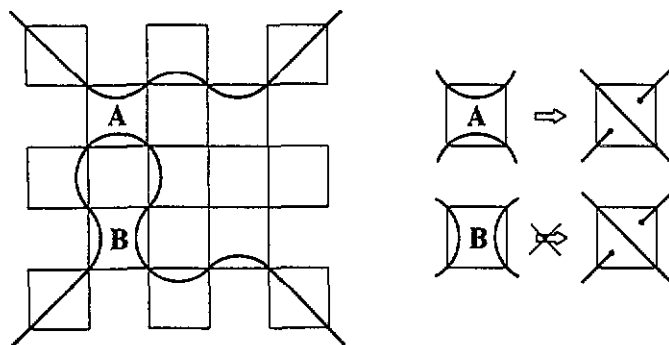


Figure A1. The schematic argument that the statistical weight of SAWs of the type $O^{(r+1)}$, which contain the lower-level walks of the type $O^{(r)}$, is smaller than the statistical weight of those walks which stem from the SAWs of the type $H^{(r+1)}$ by splitting the $H^{(r)}$ walks, that is, $b_{O|*}^O < \partial H^{(r+1)} / \partial H^{(r)}$. The argument invokes the fact that the $O^{(r+1)}$ walks of interest can be obtained from a subset of all walks of the type $H^{(r+1)}$ which contain the $H^{(r)}$ walks. Finally, one should observe that there are splittings of the $H^{(r)}$ walks (the A case) which contribute to the $O^{(r+1)}$ set, and that there are those (the B case) which do not make the appropriate contribution.

where $\alpha(0, \delta)$ is proportional to δ , that is, $\alpha(0, \delta) \sim (x^* - x)$. The requirement that (A3) and the relation (A4) can be valid for $r \leq r_0$, where r_0 is given by

$$r_0 = \frac{\ln \epsilon'}{\ln \lambda_1} \quad (\text{A5})$$

with ϵ' being equal to $\epsilon / \alpha(0, \delta)$. Knowing the counter value r_0 , we can proceed further by calculating all polynomials which appear in (3) and (4), at the fixed point (F^*, G^*, H^*) for $r \leq r_0$, and at the trivial fixed point $(0, 0, 0)$ for $r > r_0$.

On the grounds of the foregoing conclusion, we split our analysis of the recursion relations (3)–(5) into two parts. For $r \leq r_0$, equation (3) becomes

$$I^{(r+1)} = a_{II}^* I^{(r)} + a_{JJ}^* J^{(r)} + a_{IK}^* K^{(r)} \quad (\text{A6})$$

$$J^{(r+1)} = a_{JI}^* I^{(r)} + a_{JJ}^* J^{(r)} + a_{JK}^* K^{(r)} \quad (\text{A7})$$

$$K^{(r+1)} = a_{KI}^* I^{(r)} + a_{KJ}^* J^{(r)} + a_{KK}^* K^{(r)} \quad (\text{A8})$$

whose solution we search in the form

$$I^{(r)} \simeq K_I \lambda_2^r \quad J^{(r)} \simeq K_J \lambda_2^r \quad K^{(r)} \simeq K_K \lambda_2^r \quad (\text{A9})$$

where K_I, K_J , and K_K , are some constants, while λ_2 is the largest solution of (7). If the solutions of the type (A9) exist, relation (4), for $Y = O$, takes the form

$$O^{(r)} \simeq K' (\lambda_2^2)^r + K'' (b_{O|*}^O)^r \quad (\text{A10})$$

where K' and K'' are also constants. The value of $b_{O|*}^O$ is smaller than $\partial H^{(r+1)} / \partial H^{(r)}$ (see figure A1). On the other hand, in the course of our work numerical evidence has been acquired that $\partial H^{(r+1)} / \partial H^{(r)} < \lambda_2^2$, so that, for large r , (A10) reduces to

$$O^{(r)} \simeq K_0 \lambda_2^{2r} \quad (\text{A11})$$

In the same spirit, certain coefficients in the recursion relations that follow from (4), upon inserting (A6)–(A8) and (A11), can be related to the partial derivatives of the partition functions (1), yielding

$$v^{(r+1)} \simeq \lambda_2^{2r} k + \hat{T}' v^{(r)} \quad (\text{A12})$$

where $v^{(r)}$ is the vector column comprised of $L^{(r)}$, $M^{(r)}$, and $N^{(r)}$, while k is also the vector column whose elements are K_L , K_M , and K_N , and, finally, \hat{T}' is the matrix

$$\hat{T}' = \begin{pmatrix} \frac{\partial F^{(r+1)}}{\partial F^{(r)}} & \frac{\partial F^{(r+1)}}{\partial G^{(r)}} & 2 \frac{\partial F^{(r+1)}}{\partial H^{(r)}} \\ \frac{\partial G^{(r+1)}}{\partial F^{(r)}} & \frac{\partial G^{(r+1)}}{\partial G^{(r)}} & 2 \frac{\partial G^{(r+1)}}{\partial H^{(r)}} \\ \frac{1}{2} \frac{\partial H^{(r+1)}}{\partial F^{(r)}} & \frac{1}{2} \frac{\partial H^{(r+1)}}{\partial G^{(r)}} & \frac{\partial H^{(r+1)}}{\partial H^{(r)}} \end{pmatrix}^* \quad (\text{A13})$$

The matrix \hat{T}' has the same eigenvalues as the matrix \hat{T} , which means that in (A12) we can neglect the second term (because $\lambda_1 < \lambda_2^2$; see table 1). Consequently, for $r \leq r_0$, we can write

$$L^{(r)} \simeq K_1 \lambda_2^{2r} \quad M^{(r)} \simeq K_2 \lambda_2^{2r} \quad N^{(r)} \simeq K_3 \lambda_2^{2r} \quad (\text{A14})$$

where K_1 , K_2 , and K_3 , are constants. In this way we have completed the analysis of the RG transformations for $r \leq r_0$.

For $r > r_0$, the set of the RG transformations becomes simplified

$$\begin{aligned} I^{(r)} &\simeq K_I \lambda_2^{r_0} & L^{(r)} &\simeq K_L \lambda_2^{2r_0} & M^{(r)} &\simeq K_M \lambda_2^{2r_0} \\ J^{(r)} &= K^{(r)} = N^{(r)} = O^{(r)} \simeq 0 \end{aligned} \quad (\text{A15})$$

due to the fact that only the polynomials a_{II} , b_{II}^L , and b_{II}^M , which appear in (3) and (4), have non-zero constant terms. In the end, we insert (A9), (A11), (A14) and (A15), into (5), and retaining the largest term of the sum we obtain

$$C(x) \sim \left(\frac{2\lambda_2^2}{b^2 + 1} \right)^{r_0} \quad (\text{A16})$$

which together with (A5) gives (6).

References

- [1] Nienhuis B 1982 *Phys. Rev. Lett.* **49** 1062
- [2] Živić I and Milošević S 1993 *J. Phys. A: Math. Gen.* **26** 3393
- [3] Živić I, Milošević S and Stanley H E 1993 *Phys. Rev. E* **47** 2430
- [4] Dhar D 1988 *J. Physique* **49** 397
- [5] Elezović–Hadžić S and Milošević S 1992 *J. Phys. A: Math. Gen.* **25** 4095
- [6] Milošević S and Živić I 1993 *J. Phys. A: Math. Gen.* **26** 7263
- [7] Guttman A J and Torrie G M 1984 *J. Phys. A: Math. Gen.* **17** 3539
- [8] Duplantier B and Saleur H 1987 *Nucl. Phys. B* **290** [FS 20] 291
- [9] Burkhardt T and Guim I 1991 *J. Phys. A: Math. Gen.* **24** L1221
- [10] Duplantier B 1986 *Phys. Rev. Lett.* **57** 941
- [11] Douglas J, Ishinabe T, Nemirovsky A and Freed K 1993 *J. Phys. A: Math. Gen.* **26** 1835
- [12] Elezović S, Knežević M and Milošević S 1987 *J. Phys. A: Math. Gen.* **20** 1215
- [13] Milošević S and Živić I 1991 *J. Phys. A: Math. Gen.* **24** L833
- [14] Fábio D A, Aarão R and Riera R 1993 *J. Stat. Phys.* **71** 453
- [15] Tasserie M, Hansen A and Bideau D 1992 *J. Physique* **2** 2025